

# Cubic Topological Kondo Insulators

Victor Alexandrov<sup>1</sup>, Maxim Dzero<sup>2</sup> and Piers Coleman<sup>1,3</sup>

<sup>1</sup>*Center for Materials Theory, Department of Physics and Astronomy, Rutgers University, Piscataway, NJ 08854-8019, USA*

<sup>2</sup>*Department of Physics, Kent State University, Kent, OH 44242, USA and*

<sup>3</sup>*Department of Physics, Royal Holloway, University of London, Egham, Surrey TW20 0EX, UK.*

(Dated: September 5, 2018)

Current theories of Kondo insulators employ the interaction of conduction electrons with localized Kramers doublets originating from a tetragonal crystalline environment, yet all Kondo insulators are cubic. Here we develop a theory of cubic topological Kondo insulators involving the interaction of  $\Gamma_8$  spin quartets with a conduction sea. The spin quartets greatly increase the potential for strong topological insulators, entirely eliminating the weak-topological phases from the diagram. We show that the relevant topological behavior in cubic Kondo insulators can only reside at the lower symmetry X or M points in the Brillouin zone, leading to three Dirac cones with heavy quasiparticles.

PACS numbers: 72.15.Qm, 73.23.-b, 73.63.Kv, 75.20.Hr

Our classical understanding of order in matter is built around Landau’s concept of an order parameter. The past few years have seen a profound growth of interest in topological phases of matter, epitomized by the quantum Hall effect and topological band insulators, in which the underlying order derives from the non-trivial connectedness of the quantum wave-function, often driven by the presence of strong spin-orbit coupling [1–9].

One of the interesting new entries to the world of topological insulators, is the class of heavy fermion, or “Kondo insulators” [10–16]. The strong-spin orbit coupling and highly renormalized narrow bands in these intermetallic materials inspired the prediction [12] that a subset of the family of Kondo insulators will be  $Z_2$  topological insulators. In particular, the oldest known Kondo insulator  $\text{SmB}_6$  [17] with marked mixed valence character, was identified as a particularly promising candidate for a strong topological insulator (STI): a conclusion that has since also been supported by band-theory calculations [13, 16]. Recent experiments [18–20] on  $\text{SmB}_6$  have confirmed the presence of robust conducting surfaces, large bulk resistivity and a chemical potential that clearly lies in the gap providing strong support for the initial prediction.

However, despite these developments, there are still many aspects of the physics in these materials that are poorly understood. One of the simplifying assumptions of the original theory [12] was to treat the  $f$ -states as Kramer’s doublets in a tetragonal environment. In fact, the tetragonal theory predicts that strong topological insulating behavior requires large deviations from integral valence, while in practice Kondo insulators are much closer to integral valence [11]. Moreover, all known Kondo insulators have cubic symmetry, and this higher symmetry appears to play a vital role, for all apparent “Kondo insulators” of lower symmetry, such as  $\text{CeNiSn}$  [21] or  $\text{CeRu}_4\text{Sn}_6$  [22] have proven, on improving sample quality, to be semi-metals. One of the important

effects of high symmetry is the stabilization of magnetic  $f$ -quartets. Moreover, Raman [23] experiments and various band-theory studies [24, 25] that it is the Kondo screening of the magnetic quartets that gives rise to the emergence of the insulating state.

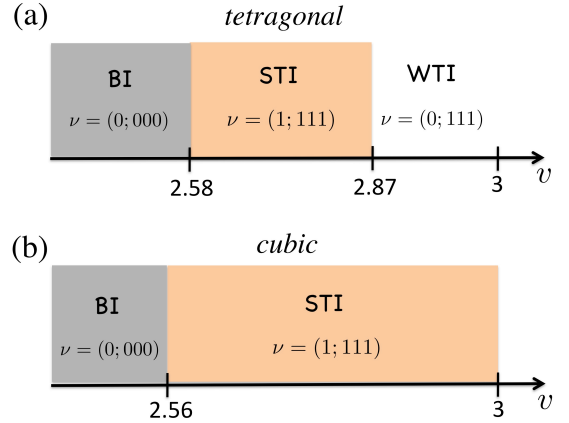


FIG. 1: Contrasting the phase diagram of tetragonal [26] and cubic topological Kondo insulators. Cubic symmetry extends the STI phase into the Kondo limit. For  $\text{SmB}_6$   $\nu = 3 - n_f$  gives the valence of the Sm ion, while  $n_f$  measures the number of  $f$ -holes in the filled  $4f^6$  state, so that  $n_f = 1$  corresponds to the  $4f^5$  configuration.

Motivated by this observation, here we formulate a theory of cubic topological Kondo insulators, based on a lattice of magnetic quartets. We show that the presence of a spin-quartet greatly increases the possibility of strong topological insulators while eliminating the weak-topological insulators from the phase diagram, Fig. 1. We predict that the relevant topological behavior in simple cubic Kondo insulators can only reside at the lower point group symmetry X and M points in the Brillouin

zone (BZ), leading to a three heavy Dirac cones at the surface. One of the additional consequences of the underlying Kondo physics, is that the coherence length of the surface states is expected to be very small, of order a lattice spacing.

While we outline our model of cubic Kondo insulators with a particular focus on  $\text{SmB}_6$ , the methodology generalizes to other cubic Kondo insulators.  $\text{SmB}_6$  has a simple cubic structure, with the  $\text{B}_6$  clusters located at the center of the unit cell, acting as spacers which mediate electron hopping between Sm sites. Band-theory [25] and XPS studies [27] show that the  $4f$  orbitals hybridize with  $d$ -bands which form electron pockets around the X points. In a cubic environment, the  $J = 5/2$  orbitals split into a  $\Gamma_7$  doublet and a  $\Gamma_8$  quartet, while the fivefold degenerate  $d$ -orbitals are split into double degenerate  $e_g$  and triply degenerate  $t_{2g}$  orbitals. Band theory and Raman spectroscopy studies [23] indicate that the physics of the  $4f$  orbitals is governed by valence fluctuations involving electrons of the  $\Gamma_8$  quartet and the conduction  $e_g$  states,  $e^- + 4f^5(\Gamma_8^{(\alpha)}) \rightleftharpoons 4f^6$ . The  $\Gamma_8^{(\alpha)}$  ( $\alpha = 1, 2$ ) quartet consists of the following combination of orbitals:  $|\Gamma_8^{(1)}\rangle = \sqrt{\frac{5}{6}}|\pm\frac{5}{2}\rangle + \sqrt{\frac{1}{6}}|\mp\frac{3}{2}\rangle$ ,  $|\Gamma_8^{(2)}\rangle = |\pm\frac{1}{2}\rangle$ . This then leads to a simple physical picture in which the  $\Gamma_8$  quartet of  $f$ -states hybridizes with an  $e_g$  quartet (Kramers plus orbital degeneracy) of  $d$ -states to form a Kondo insulator.

To gain insight into how the cubic topological Kondo insulator emerges it is instructive to consider a simplified one-dimensional model consisting of a quartet of conduction  $d$ -bands hybridized with a quartet of  $f$ -bands (Fig. 2a). In one dimension there are two high symmetry points:  $\Gamma$  ( $k = 0$ ) and X ( $k = \pi$ ), where the hybridization vanishes [12, 14, 26]). Away from the zone center  $\Gamma$ , the  $f$ - and  $d$ - quartets split into Kramers doublets. The  $Z_2$  topological invariant  $\nu_{1D}$  is then determined by the product of the parities  $\nu_{1D} = \delta_\Gamma \delta_X$  of the occupied states at the  $\Gamma$  and X points. However, the  $f$ -quartet at the  $\Gamma$  point is equivalent to two Kramers doublets, which means that  $\delta_\Gamma = (\pm 1)^2$  is always positive, so that  $\nu_{1D} = \delta_X$  and a one-dimensional topological insulator only develops when the  $f$  and  $d$  bands invert at the X point.

Generalizing this argument to three dimensions we see that there are now four high symmetry points  $\Gamma$ , X, M and R. The  $f$ -bands are fourfold degenerate at both  $\Gamma$  and R points which guarantees that  $\delta_\Gamma = \delta_R = +1$  (Fig. 2b). Therefore, we see that the 3D topological invariant is determined by band inversions at X or M points only,  $\nu_{3D} = (\delta_X \delta_M)^3 = \delta_X \delta_M$ . If there is a band inversion at the X point, we get  $\nu_{3D} = \delta_X \delta_M = -1$ . In this way the cubic character of the Kondo insulator and, specifically, the fourfold degeneracy of the  $f$ -orbital multiplet protects the formation of a strong topological insulator.

We now formulate our model for cubic topological

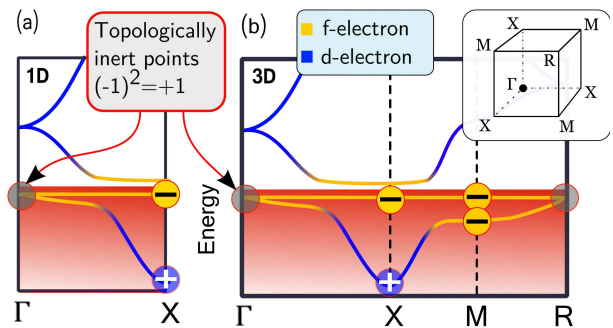


FIG. 2: Schematic band structure illustrating (a) 1D Kondo insulator with local cubic symmetry and (b) 3D cubic Kondo insulator. Hybridization between a quartet of  $d$ -bands with a quartet of  $f$ -bands leads to a Kondo insulator. The fourfold degeneracy of the  $f$ - and  $d$ -bands at the high symmetry  $\Gamma$  and R points of the Brillouin zone guarantees that the 3D topological invariant is determined by the band inversions at the X and M points only.

Kondo insulators. At each site, the quartet of  $f$  and  $d$ -holes is described by an orbital and spin index, denoted by the combination  $\lambda \equiv (a, \sigma)$  ( $a = 1, 2$ ,  $\sigma = \pm 1$ ). The fields are then given by the eight component spinor

$$\Psi_j = \begin{pmatrix} d_\lambda(j) \\ X_{0\lambda}(j) \end{pmatrix} \quad (1)$$

where  $d_\lambda(j)$  destroys an  $d$ -hole at site  $j$ , while  $X_{0\lambda}(j) = |4f^6\rangle\langle 4f^5, \lambda|$  is the Hubbard operator that destroys an  $f$ -hole at site  $j$ . The tight-binding Hamiltonian describing the hybridized  $f$ - $d$  system is then

$$H = \sum_{i,j} \Psi_\lambda^\dagger(i) h_{\lambda\lambda'}(\mathbf{R}_i - \mathbf{R}_j) \Psi_{\lambda'}(j) \quad (2)$$

in which the nearest hopping matrix has the structure

$$h(\mathbf{R}) = \begin{pmatrix} h^d(\mathbf{R}) & V(\mathbf{R}) \\ V^\dagger(\mathbf{R}) & h^f(\mathbf{R}) \end{pmatrix}, \quad (3)$$

where the diagonal elements describe hopping within the  $d$ - and  $f$ - quartets while the off-diagonal parts describe the hybridization between them, while  $\mathbf{R} \in (\pm\hat{x}, \pm\hat{y}, \pm\hat{z})$  is the vector linking nearest neighbors. The various matrix elements simplify for hopping along the  $z$ -axis, where they become orbitally and spin diagonal:

$$h^l(\mathbf{z}) = t^l \begin{pmatrix} 1 \\ \eta_l \end{pmatrix}, \quad V(\mathbf{z}) = iV \begin{pmatrix} 0 \\ \sigma_z \end{pmatrix}. \quad (4)$$

where  $l = d, f$  and  $\eta_l$  is the ratio of orbital hopping elements. In the above, the overlap between the  $\Gamma_8^{(1)}$  orbitals, which extend perpendicular to the  $z$ -axis is neglected, since the hybridization is dominated by the overlap of the  $\Gamma_8^{(2)}$  orbitals, which extend out along the  $z$ -axis. The hopping matrix elements in the  $x$  and  $y$  directions are then obtained by rotations in orbital/spin

space. so that  $h(\mathbf{x}) = U_y h(\mathbf{z}) U_y^\dagger$  and  $h(\mathbf{y}) = U_{-x} h(\mathbf{z}) U_{-x}^\dagger$  where  $U_y$  and  $U_{-x}$  denote 90° rotations about the y and negative x axes, respectively.

The Fourier transformed hopping matrices  $h(\mathbf{k}) = \sum_{\mathbf{R}} h(\mathbf{R}) e^{-i\mathbf{k}\cdot\mathbf{R}}$  can then be written in the compact form

$$h^l(\mathbf{k}) = t^l \begin{pmatrix} \phi_1(\mathbf{k}) + \eta_l \phi_2(\mathbf{k}) & (1 - \eta_l) \phi_3(\mathbf{k}) \\ (1 - \eta_l) \phi_3(\mathbf{k}) & \phi_2(\mathbf{k}) + \eta_l \phi_1(\mathbf{k}) \end{pmatrix} + \epsilon^l, \quad (5)$$

where  $l = d, f$ . Here  $\epsilon^l$  are the bare energies of the isolated d and f-quartets, while  $\phi_1(\mathbf{k}) = c_x + c_y + 4c_z$ ,  $\phi_2(\mathbf{k}) = 3(c_x + c_y)$  and  $\phi_3(\mathbf{k}) = \sqrt{3}(c_x - c_y)$  ( $c_\alpha \cos k_\alpha, \alpha = x, y, z$ ). The hybridization is given by

$$V(\mathbf{k}) = \frac{1}{6} \begin{pmatrix} 3(\bar{\sigma}_x + i\bar{\sigma}_y) & \sqrt{3}(\bar{\sigma}_x - i\bar{\sigma}_y) \\ \sqrt{3}(\bar{\sigma}_x - i\bar{\sigma}_y) & \bar{\sigma}_x + i\bar{\sigma}_y + 4\bar{\sigma}_z \end{pmatrix} \quad (6)$$

where we denote  $\bar{\sigma}_\alpha = \sigma_\alpha \sin k_\alpha$ . Note how the hybridization between the even parity d-states and odd-parity f-states is an odd parity function of momentum  $V(\mathbf{k}) = -V(-\mathbf{k})$ .

To analyze the properties of the Kondo insulator, we use a slave boson formulation of the Hubbard operators, writing  $X_{\lambda 0}(j) = f_\lambda^\dagger(j) b_j$ , where  $f_\lambda^\dagger|0\rangle \equiv |4f^5, \lambda\rangle$  creates an f-hole in the  $\Gamma^8$  quartet while  $b^\dagger|0\rangle \equiv |4f^6\rangle$  denotes the singlet filled 4f shell, subject to the constraint  $Q_j = b_j^\dagger b_j + \sum_\lambda f_{j\lambda}^\dagger f_{j\lambda} = 1$  at each site.

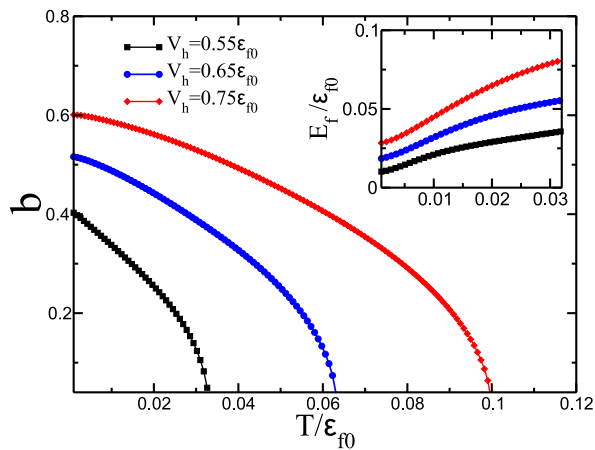


FIG. 3: Temperature dependence of the hybridization gap parameter  $b$  and the renormalized  $f$ -level position (inset) for various values of the bare hybridization (see Supplementary Materials for more details).

We now analyze the properties of the cubic Kondo insulator, using a mean-field treatment of the slave boson field  $b_i$ , replacing the slave-boson operator  $\hat{b}_i$  at each site by its expectation value:  $\langle \hat{b}_i \rangle = b$  so that the f-hopping and hybridization amplitude are renormalized:  $t_f \rightarrow b^2 t_f$  and  $V_{df} \rightarrow b V_{df}$ . The mean-field theory is carried out, enforcing the constraint  $b^2 + \langle n_f \rangle = 1$  on the average. In addition, the chemical potentials  $\epsilon_d$  and  $\epsilon_f$  for both  $d$ -electrons and  $f$ -holes are adjusted self-consistently to

produce a band insulator,  $n_d + n_f = 4$ . This condition guarantees that four out of eight doubly degenerate bands will be fully occupied. The details of our mean-field calculation are given in the Supplementary Materials section. Here we provide the final results of our calculations.

In Fig. 3 we show that the magnitude  $b$  reduces with temperature, corresponding to a gradual rise in the Sm valence, due to the weaker renormalization of the  $f$ -electron level. The degree of mixed valence of  $\text{Sm}^+$  is given then by  $v = 3 - \langle n_f \rangle$ . In our simplified mean-field calculation, the smooth temperature cross-over from Kondo insulating behavior to local moment metal at high temperatures is crudely approximated by an abrupt second-order phase transition.

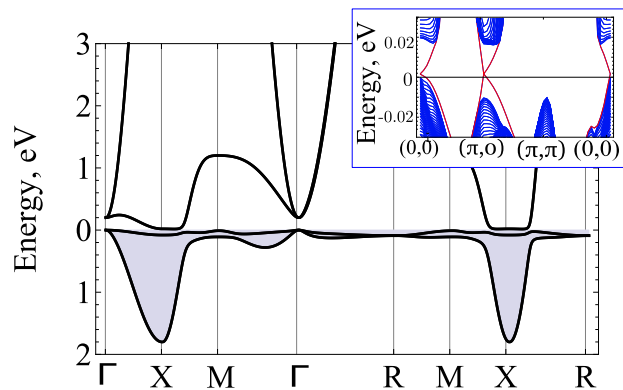


FIG. 4: Band structure consistent with PES and LDA studies of  $\text{SmB}_6$  computed with the following parameters:  $n_f = 0.48$  (or  $b = 0.73$ ),  $V = 0.05$  eV,  $t_d = 2$  eV,  $\mu_d = 0.2$  eV,  $\eta = \eta' = -0.3$ ,  $\epsilon_f = -0.01$  eV ( $\epsilon_{f0} = -0.17$  eV),  $t_f = -0.05$  eV,  $T = 10^{-4}$  eV and the gap is  $\Delta = 12$  meV. Shaded region denotes filled bands. Inset shows the ground-state energy computed for a slab of 80 layers to illustrate the three gapless surface Dirac excitations at the symmetry points  $\hat{\Gamma}$ ,  $\hat{X}'$  and  $\hat{X}''$ .

Fig. 4 shows the computed band structure for the cubic Kondo insulator obtained from mean-field theory, showing the band inversion between the  $d$ - and  $f$ -bands at the X points that generates the strong topological insulator. Moreover, as the value of the bare hybridization increases, there is a maximum value beyond which the bands no longer invert and the Kondo insulator becomes a conventional band insulator.

One of the interesting questions raised by this work concerns the many body character of the Dirac electrons on the surface. Like the low-lying excitations in the valence and conduction band, the surface states of a TKI involve heavy quasiparticles of predominantly  $f$ -character. The characteristic Fermi velocity of these excitations  $v_F^* = Z v_F$  is renormalized with respect to the conduction electron band group velocities, where  $Z = m/m^*$  is the mass renormalization of the  $f$ -electrons. In a band topological insulator, the penetration depth of the sur-

face states  $\xi \sim v_F/\Delta$ , where  $\Delta$  is the band-gap, scale that is significantly larger than a unit-cell size. Paradoxically, even though the Fermi velocity of the Dirac cones in a TKI is very low, we expect the characteristic penetration depth  $\xi$  of the heavy wavefunctions into the bulk to be of order the lattice spacing  $a$ . To see this, we note that  $\xi \sim \frac{v_F^*}{\Delta_g}$ , where the indirect gap of the Kondo insulator  $\Delta_g$  is of order the Kondo temperature  $\Delta_g \sim T_K$ . But since  $T_K \sim ZW$ , where  $W$  is the width of the conduction electron band, this implies that the penetration depth of the surface excitations  $\xi \sim v_F/W \sim a$  is given by the size  $a$  of the unit cell. Physically, we can interpret the surface Dirac cones as a result of broken Kondo singlets, whose spatial extent is of order a lattice spacing. This feature is likely to make the surface states rather robust against the purity of the bulk.

Various interesting questions are raised by our study. Conventional Kondo insulators are most naturally understood as a strong-coupling limit of the Kondo lattice, where local singlets form between a commensurate number of conduction electrons and localized moments. What then is the appropriate strong coupling description of topological Kondo insulators, and can we understand the surface states in terms of broken Kondo singlets? A second question concerns the temperature dependence of the hybridization gap. Experimentally, the hybridization gap observed in Raman studies[23] is seen to develop in a fashion strongly reminiscent of the mean-field theory. Could this indicate that fluctuations about mean-field theory are weaker in a fully gapped Kondo lattice than in its metallic counterpart?

We end with a few comments on the experimental consequences of the above picture. One of the most dramatic consequences of the quartet model is the prediction of three Dirac cones of surface excitation of substantially enhanced effective mass. By contrast, were the underlying ground-state of the f-state a Kramers doublet, then we would expect a single Dirac cone excitation. These surface modes should be observable via various low energy spectroscopies. For instance, the heavy mass of the quasi particles should appear in Shubnikov-de Haas or cyclotron resonance measurements. The quasiparticle mass  $m^* = \hbar k_F/v_F^* \sim m_e(k_F a)Z^{-1}$  will depend on the Fermi momentum  $k_F$  of the Dirac cones. Scanning tunneling spectroscopy measurements of the quasiparticle interference created by the Dirac cones, and high resolution ARPES measurements may provide a direct way to observe the predicted three Dirac cones.

To summarize, we have studied the cubic topological Kondo insulator, incorporating the effect of a fourfold degenerate  $f$ -multiplet. There are two main effects of the quartet states: first, they allow the low fractional filling of the band required for strong topological insulating behavior to occur in the almost integral valent environment of the Kondo insulator; second, they double the degeneracy

of the band-states at the high-symmetry  $\Gamma$  and  $R$  points in the Brillouin zone, removing these points from the calculation of the  $Z_2$  topological invariant so that the only important band crossings occur at the the X or M points. This leads to a prediction that three heavy Dirac cones will form on the surfaces [13, 16].

We would like to thank A. Ramires, V. Galitski, K. Sun, S. Artyukhin and J. P. Paglione for stimulating discussions related to this work. This work was supported by the Ohio Board of Regents Research Incentive Program grant OBR-RIP-220573 (M.D.), DOE grant DE-FG02-99ER45790 (V. A & P. C.), the U.S. National Science Foundation I2CAM International Materials Institute Award, Grant DMR-0844115.

- 
- [1] L. Fu, C. L. Kane and E. J. Mele, Phys. Rev. Lett. **98**, 106803 (2007).
  - [2] J. E. Moore and L. Balents, Phys. Rev. B **75**, 121306(R) (2007).
  - [3] D. Hsieh, D. Qian, L. Wray, Y. Xia, Y. S. Hor, R. J. Cava and M. Z. Hasan, Nature **452**, 970 (2008).
  - [4] Y. Xia, D. Qian, D. Hsieh, L. Wray, A. Pal, H. Lin, A. Bansil, D. Grauer, Y. S. Hor, R. J. Cava and M. Z. Hasan, Nat. Phys. **5**, 398 (2009).
  - [5] P. Roushan, J. Seo, C. V. Parker, Y. S. Hor, D. Hsieh, D. Qian, A. Richardella, M. Z. Hasan, R. J. Cava and A. Yazdani, Nature **460**, 1106 (2009).
  - [6] T. Zhang, P. Cheng, X. Chen, J. F. Jia, X. C. Ma, K. He, L. L. Wang, H. J. Zhang, X. Dai, Z. Fang, X. C. Xie and Q. K. Xue, Phys. Rev. Lett. **103**, 266803 (2009).
  - [7] J. Seo, P. Roushan, H. Beidenkopf, Y. S. Hor, R. J. Cava, and A. Yazdani, Nature **466**, 343 (2010).
  - [8] M. Z. Hasan and C.L. Kane, Rev. Mod. Phys. **82**, 3045 (2010).
  - [9] X.-L. Qi and S.-C. Zhang, Rev. Mod. Phys. **83**, 1057 (2011).
  - [10] G. Aeppli & Z. Fisk, Comm. Condens. Matter Phys. **16**, 155 (1992).
  - [11] P. Riseborough, Adv. Phys. **49**, 257 (2000).
  - [12] M. Dzero, K. Sun, V. Galitski and P. Coleman, Phys. Rev. Lett. **104**, 106408 (2010).
  - [13] T. Takimoto, J. Phys. Soc. Jpn. **80**, 123710 (2011).
  - [14] M. Dzero, K. Sun, P. Coleman and V. Galitski, Phys. Rev. B **85**, 045130 (2012).
  - [15] M. T. Tran, T. Takimoto, and K. S. Kim, Phys. Rev. B **85**, 125128 (2012).
  - [16] F. Lu, J. Zhao, H. Weng, Z. Fang and X. Dai, Phys. Rev. Lett. **110**, 096401 (2013).
  - [17] A. Menth, E. Buehler & T. H. Geballe, Phys. Rev. Lett. **22**, 295 (1969).
  - [18] S. Wolgast, C. Kurdak, K. Sun, J. W. Allen, D. J. Kim and Z. Fisk, pre-print arXiv:1211.5104 (2012).
  - [19] X. Zhang, N. P. Butch, P. Syers, S. Ziemak, R. L. Greene, and J. P. Paglione, Phys. Rev. X **3**, 011011 (2013) Phys. Rev. X **3**, 011011 (2013).
  - [20] J. Botimer, D. J. Kim, S. Thomas, T. Grant, Z. Fisk and J. Xin, pre-print arXiv:1211.6769 (2012).
  - [21] K. Izawa, T. Suzuki, T. Fujita, T. Takabatake, G.

- Nakamoto, H. Fujii and K. Maetzawa, Phys. Rev. **B** 59, 2599 (1999).
- [22] S. Paschen, H. Winkler, T. Nezu, M. Kriegisch, G. Hilscher, J. Custers, and A. Prokofiev, J. Phys: Conf. Ser 200, 012156 (2010).
- [23] P. Nyhus, S. L. Cooper, Z. Fisk and J. Sarrao, Phys. Rev. **B** 55, 12488 (1997).
- [24] A. Yanase and H. Harima, Prog. Theor. Phys. Suppl. **108**, 19 (1992).
- [25] V. N. Antonov, B. Harmon and A. N. Yaresko, Phys. Rev. **B** 66, 165209 (2002).
- [26] M. Dzero, Eur. Phys. J. **B** 85, 297 (2012).
- [27] H. Miyazaki, Tesuya Hajiri, T. Ito, S. Kunii and S. Kimura, Phys. Rev. **B** 86, 075105 (2012).

**SUPPLEMENTARY MATERIALS FOR CUBIC TOPOLOGICAL KONDO INSULATORS**

These notes provide:

- details of the derivation of the tight-binding Hamiltonian for a cubic Kondo insulator.
- derivation of the mean-field theory for the infinite  $U$  limit
- derivation of the mean-field equations.

**Rotation matrices**

To construct the Hamiltonian, we evaluate the hopping matrices along the  $z$ -axis, and then carry out a unitary transformation to evaluate the corresponding quantities for hopping along the  $x$  and  $y$  axes.

Consider a general rotation operator

$$\mathcal{R} = R\Lambda, \quad (7)$$

where  $R$  and  $\Lambda$  describe  $\pi/2$  rotations about a principle axis of the crystal in real and spin space respectively. The Hamiltonian in a cubic environment is invariant under these transformations:  $H = \mathcal{R}^\dagger H \mathcal{R}$ . We now write the directional dependence of the Hamiltonian explicitly.

$$H(x, y, z) = (R\Lambda)^\dagger H(x, y, z) R\Lambda = \Lambda^\dagger (R^\dagger H(x, y, z) R) \Lambda. \quad (8)$$

We can always choose the rotation  $\mathcal{R}$  to transform in the cyclic manner:  $x \rightarrow y \rightarrow z \rightarrow x$ , then substituting  $z = y = 0$ ,

$$H(x, 0, 0) = \Lambda^\dagger (R_x^\dagger H(x, 0, 0) R_x) \Lambda = \Lambda_x^\dagger H(0, 0, x) \Lambda, \quad (9)$$

hence we can assume the 3D Hamiltonian of the following form

$$H_{3D} = H(k_z) + \Lambda H(k_x) \Lambda^\dagger + \Lambda^\dagger H(k_y) \Lambda, \quad (10)$$

Where to rotate in the opposite direction we use  $\Lambda^{-1} = \Lambda^\dagger$ . Using the Wigner D-functions we can construct the rotation in angular momentum space

$$\Lambda = e^{-i\alpha J_z} e^{-i\beta J_y} e^{-i\gamma J_z}. \quad (11)$$

Here,  $\Lambda$  denotes the rotation operator in the "ZYZ" convention, corresponding to a rotation around the  $z$ -axis, followed by a rotation around the  $y$ -axis, and then the new  $z$ -axis. The matrix elements of this operator are then

$$\begin{aligned} D_{m'm}^J &= \langle Jm' | \Lambda | Jm \rangle \\ &= [(j+m)!(j-m)!(j+m')!(j-m')!]^{1/2} \\ &\quad \times \sum_{\chi} \frac{(-1)^\chi}{(j-m'-\chi)!(j+m-\chi)!(\chi+m'-m)! \chi!} \\ &\quad \times \left( \cos \frac{\beta}{2} \right)^{2j+m-m'-2\chi} \left( -\sin \frac{\beta}{2} \right)^{m'-m+2\chi} \\ &\quad \times e^{-im'\alpha - im\gamma} \end{aligned}$$

so that upon rotating the state  $|Jm\rangle$  using  $R_x$  we obtain  $\Lambda^{(j=5/2)} = D_{mm'}^{5/2}(0, \pi/2, \pi/2)$ , and  $\Lambda^{(j=2)} = D_{mm'}^2 \otimes D_{mm'}^{1/2}(0, \pi/2, \pi/2)$ . One can now obtain the transformation matrices for a given multiplet ( $e_g, t_{2g}, \Gamma_8$  etc). For the  $e_g$  doublet we are to read off the matrices  $M_{ij} = \langle i | \Lambda_x | j \rangle$  from the transformation equation

$$\Lambda_x |e_g : m\rangle = |e_g : n\rangle M_{nm}^d, \quad (12)$$

where  $|e_g : m\rangle \equiv \{|d_{x^2-y^2} \uparrow\rangle, |d_{z^2} \uparrow\rangle, |d_{x^2-y^2} \downarrow\rangle, |d_{z^2} \downarrow\rangle\}$  is an  $e_g$  doublet. Similarly for the  $\Gamma_8$  quartet,

$$\Lambda_x |\Gamma_8, \alpha\rangle = |\Gamma_8, \beta\rangle M_{\beta\alpha}^f, \quad (13)$$

where the quartet is denoted by  $|\Gamma_8, \alpha\rangle$ , where  $\alpha \in [1, 4]$ . The result is,

$$M_{mn}^d = e^{\frac{i3\pi}{4}} \begin{pmatrix} \frac{i}{2\sqrt{2}} & \frac{1}{2}i\sqrt{\frac{3}{2}} & -\frac{i}{2\sqrt{2}} & -\frac{1}{2}i\sqrt{\frac{3}{2}} \\ -\frac{1}{2}i\sqrt{\frac{3}{2}} & \frac{i}{2\sqrt{2}} & \frac{1}{2}i\sqrt{\frac{3}{2}} & -\frac{i}{2\sqrt{2}} \\ \frac{1}{2\sqrt{2}} & \frac{\sqrt{\frac{3}{2}}}{2} & \frac{1}{2\sqrt{2}} & \frac{\sqrt{\frac{3}{2}}}{2} \\ -\frac{\sqrt{\frac{3}{2}}}{2} & \frac{1}{2\sqrt{2}} & -\frac{\sqrt{\frac{3}{2}}}{2} & \frac{1}{2\sqrt{2}} \end{pmatrix}, \quad M_{\alpha\beta}^f = e^{\frac{i3\pi}{4}} \begin{pmatrix} \frac{1}{2\sqrt{2}} & \frac{\sqrt{\frac{3}{2}}}{2} & -\frac{1}{2\sqrt{2}} & -\frac{\sqrt{\frac{3}{2}}}{2} \\ -\frac{\sqrt{\frac{3}{2}}}{2} & \frac{1}{2\sqrt{2}} & \frac{\sqrt{\frac{3}{2}}}{2} & -\frac{1}{2\sqrt{2}} \\ -\frac{i}{2\sqrt{2}} & -\frac{1}{2}i\sqrt{\frac{3}{2}} & -\frac{i}{2\sqrt{2}} & -\frac{1}{2}i\sqrt{\frac{3}{2}} \\ \frac{1}{2}i\sqrt{\frac{3}{2}} & -\frac{i}{2\sqrt{2}} & \frac{1}{2}i\sqrt{\frac{3}{2}} & -\frac{i}{2\sqrt{2}} \end{pmatrix}. \quad (14)$$

Note that the rotation cyclically exchanges  $x \rightarrow y \rightarrow z \rightarrow x$ , thus applying it three times gives overall "−1" due to fermionic statistics.

$$M^3 = -1.$$

Finally, we can use (14) to derive the hamiltonian defined in (5) and (6) of the main paper.

### Details of the mean-field theory

The full Hamiltonian for the problem also contains a term describing the local Hubbard interaction between the  $f$ -electrons:

$$H_f = U \sum_i \sum_{\alpha=1}^4 \sum_{\beta \neq \alpha} f_{i\alpha}^\dagger f_{i\alpha} f_{i\beta}^\dagger f_{i\beta} \quad (15)$$

We consider the infinite  $U$ , where we can project out all states with occupation number larger than one by replacing the bare  $f$ -electron fields by Hubbard operators. We represent the Hubbard operators using a slave boson representation, as follows:

$$f_{i\alpha}^\dagger \rightarrow X_{\alpha 0}(i) = f_{i\alpha}^\dagger b_i, \quad f_{i\alpha} \rightarrow X_{0\alpha}(i) = b_i^\dagger f_{i\alpha}, \quad (16)$$

supplemented by a constraint of no more than one  $f$ -electron per each site ( $U = \infty$ ):

$$\sum_{\alpha=1}^4 f_{i\alpha}^\dagger f_{i\alpha} + b_i^\dagger b_i = 1. \quad (17)$$

The partition function corresponding to the model Hamiltonian  $H = H_c + H_f + H_{hyb}$  above and with constraint condition (17) reads :

$$Z = \int_{-\pi/\beta}^{\pi/\beta} \frac{\beta d\lambda}{\pi} \int \mathcal{D}(b, b^\dagger, f, f^\dagger, c, c^\dagger) \exp \left( - \int_0^\beta L(\tau) d\tau \right), \quad (18)$$

where the Lagrangian  $L(\tau)$  is

$$L = \sum_i b_i^\dagger \frac{d}{d\tau} b_i + \sum_{ij} \sum_{\alpha, \beta=1}^4 f_{i\alpha}^\dagger \left[ \delta_{ij} \delta_{\alpha\beta} \left( \frac{d}{d\tau} + \varepsilon_f \right) + b_i^\dagger \overset{(f)}{t}_{ij, \alpha\beta} b_j^\dagger \right] f_{j\beta} + \sum_{\mathbf{k}\sigma} \sum_{a, b=1}^2 c_{\mathbf{a}\mathbf{k}\sigma}^\dagger \left( \frac{d}{d\tau} + \varepsilon_{ab}^{(d)}(\mathbf{k}) \right) c_{b\mathbf{k}\sigma} \\ + \frac{1}{2} \sum_{\langle ij \rangle} \sum_{\mathbf{k}\sigma} \sum_{a=1}^2 \sum_{\beta=1}^4 \left( V_{ia\sigma, j\beta} c_{a\mathbf{i}\sigma}^\dagger b_i^\dagger f_{j\beta} + \text{h.c.} \right) + \sum_j i\lambda_j \left( \sum_{\alpha=1}^4 f_{j\alpha}^\dagger f_{j\alpha} + b_j^\dagger b_j - 1 \right) \quad (19)$$

Mean-field (saddle-point) approximation corresponds to the following values of the bosonic fields:

$$b_{\mathbf{q}}(\tau) = b \delta_{\mathbf{q}, 0}, \quad i\lambda_{\mathbf{q}}(\tau) = (E_f - \varepsilon_f) \delta_{\mathbf{q}, 0}, \quad (20)$$

where both  $a$  and  $\varepsilon_f$  are  $\tau$ -independent. In the mean-field theory we choose a "radial" gauge where the phase of the  $b$ -field has been absorbed into the  $f$ -electron fields. Also, for an insulator, we need a filled quartet of states at each site, so that

$$n_c + n_f = 4. \quad (21)$$

Note, the parameter  $b$  also renormalizes the  $f$ -hopping elements. Indeed, it follows that when  $i \neq j$ ,  $f_{i\alpha}^\dagger f_{j\beta} \rightarrow X_{\alpha 0}(i)X_{0\beta}(j) = f_{i\alpha}^\dagger b_i b_j^\dagger f_{j\beta}$ . However, the onsite occupancy is unrenormalized by the slave boson fields, since in the infinite  $U$  limit, the onsite occupancy  $X_{\alpha\alpha}(i) = f_{i\alpha}^\dagger f_{i\alpha}$ .

The first three terms together with the last term in the Lagrangian (19) can be written using the new fermionic basis and (20). It follows:

$$L_0(\tau) = (b^2 - 1)(E_f - \varepsilon_f) + \sum_{\mathbf{k}\alpha} \sum_{n=1}^2 \tilde{f}_{n\mathbf{k}\alpha}^\dagger \left( \frac{d}{d\tau} + E_{n\mathbf{k}}^{(f)} \right) \tilde{f}_{n\mathbf{k}\alpha} + \sum_{\mathbf{k}\sigma} \sum_{a=1}^2 d_{a\mathbf{k}\sigma}^\dagger \left( \frac{d}{d\tau} + E_{a\mathbf{k}}^{(d)} \right) d_{a\mathbf{k}\sigma} \quad (22)$$

where the renormalized  $f$ -electron dispersion is

$$E_{n\mathbf{k}}^{(f)} = E_f + 2t_f b^2 \left( c_x + c_y + c_z + (-1)^n \sqrt{c_x^2 + c_y^2 + c_z^2 - c_x c_y - c_y c_z - c_z c_x} \right), \quad n = 1, 2. \quad (23)$$

Correspondingly, the hybridization matrix in the new fermionic basis can be obtained via unitary transformation with the matrix

$$\mathcal{U}_{\mathbf{k}} = \begin{pmatrix} u_{\mathbf{k}} & 0 & v_{\mathbf{k}} & 0 \\ 0 & u_{\mathbf{k}} & 0 & v_{\mathbf{k}} \\ -v_{\mathbf{k}} & 0 & u_{\mathbf{k}} & 0 \\ 0 & -v_{\mathbf{k}} & 0 & u_{\mathbf{k}} \end{pmatrix}, \quad \mathcal{U}_{\mathbf{k}}^{-1} = \begin{pmatrix} u_{\mathbf{k}} & 0 & -v_{\mathbf{k}} & 0 \\ 0 & u_{\mathbf{k}} & 0 & -v_{\mathbf{k}} \\ v_{\mathbf{k}} & 0 & u_{\mathbf{k}} & 0 \\ 0 & v_{\mathbf{k}} & 0 & u_{\mathbf{k}} \end{pmatrix}. \quad (24)$$

Thus we need to calculate the elements of the matrix

$$\tilde{H}_V = iV_{df} \frac{b}{2} \sum_{\mathbf{k}} \tilde{d}_{\mathbf{k}}^\dagger \mathcal{U}_{\mathbf{k}}^{-1} H_{hyb}(\mathbf{k}) \mathcal{U}_{\mathbf{k}} \tilde{f}_{\mathbf{k}} + \text{h.c.} \quad (25)$$

We can use the following relations

$$u_{\mathbf{k}}^2 - v_{\mathbf{k}}^2 = \frac{c_x + c_y - 2c_z}{2R_{\mathbf{k}}}, \quad u_{\mathbf{k}} v_{\mathbf{k}} = \frac{\sqrt{3}}{4R_{\mathbf{k}}} (c_x - c_y). \quad (26)$$

In our subsequent discussion it will be convenient to write  $\tilde{H}_V(\mathbf{k})$  in a more compact form. To derive the corresponding expression we first recall that  $H_{hyb}$  can be written as follows

$$H_{hyb}(\mathbf{k}) = iV_{df} \frac{b}{2} \left[ \hat{\phi}^x(\mathbf{k}) \otimes \hat{\sigma}_x + \hat{\phi}^y(\mathbf{k}) \otimes \hat{\sigma}_y + \hat{\phi}^z(\mathbf{k}) \otimes \hat{\sigma}_z \right], \quad \hat{\phi}_\alpha = \phi_0^\alpha \hat{\tau}_0 + \phi_1^\alpha \hat{\tau}_z + \phi_2^\alpha \hat{\tau}_x, \quad (27)$$

$$\vec{\phi}_0 = \frac{2}{3}(\sin k_x, -\sin k_y, \sin k_z), \quad \vec{\phi}_1 = \frac{1}{3}(\sin k_x, -\sin k_y, -2\sin k_z), \quad \vec{\phi}_2 = +\frac{1}{\sqrt{3}}(\sin k_x, \sin k_y, 0).$$

Again, note the change from minus sign to plus sign in front of  $\vec{\phi}_2$  term. This yields the agreement with the hybridization Hamiltonian obtained from the rotations method. We also have

$$\hat{\mathcal{U}}_{\mathbf{k}} = u_{\mathbf{k}} \hat{\tau}_0 \otimes \hat{\sigma}_0 + i v_{\mathbf{k}} \hat{\tau}_y \otimes \hat{\sigma}_0, \quad \hat{\mathcal{U}}_{\mathbf{k}}^{-1} = u_{\mathbf{k}} \hat{\tau}_0 \otimes \hat{\sigma}_0 - i v_{\mathbf{k}} \hat{\tau}_y \otimes \hat{\sigma}_0, \quad (28)$$

After some algebra we find

$$\begin{aligned} \hat{\mathcal{U}}_{\mathbf{k}}^{-1} (\hat{\tau}_0 \otimes \hat{\sigma}_x) \hat{\mathcal{U}}_{\mathbf{k}} &= \hat{\tau}_0 \otimes \hat{\sigma}_x, \\ \hat{\mathcal{U}}_{\mathbf{k}}^{-1} (\hat{\tau}_z \otimes \hat{\sigma}_x) \hat{\mathcal{U}}_{\mathbf{k}} &= (u_{\mathbf{k}}^2 - v_{\mathbf{k}}^2) (\hat{\tau}_z \otimes \hat{\sigma}_x) + 2u_{\mathbf{k}} v_{\mathbf{k}} (\hat{\tau}_x \otimes \hat{\sigma}_x), \\ \hat{\mathcal{U}}_{\mathbf{k}}^{-1} (\hat{\tau}_x \otimes \hat{\sigma}_x) \hat{\mathcal{U}}_{\mathbf{k}} &= (u_{\mathbf{k}}^2 - v_{\mathbf{k}}^2) (\hat{\tau}_x \otimes \hat{\sigma}_x) - 2u_{\mathbf{k}} v_{\mathbf{k}} (\hat{\tau}_z \otimes \hat{\sigma}_x). \end{aligned} \quad (29)$$

These results become much more transparent if we express  $u_{\mathbf{k}}$  and  $v_{\mathbf{k}}$  in terms of the angle  $\theta_{\mathbf{k}}$ :

$$u_{\mathbf{k}} = \cos(\theta_{\mathbf{k}}/2), \quad v_{\mathbf{k}} = \sin(\theta_{\mathbf{k}}/2). \quad (30)$$

Then we see that

$$\hat{\mathcal{U}}_{\mathbf{k}}^{-1} \left( \hat{\phi}^x(\mathbf{k}) \otimes \hat{\sigma}_x \right) \hat{\mathcal{U}}_{\mathbf{k}} = \hat{\Phi}^x(\mathbf{k}) \otimes \hat{\sigma}_x, \quad (31)$$



where now

$$\hat{\Phi}^x = \Phi_0^x \hat{\tau}_0 + \Phi_1^x \hat{\tau}_z + \Phi_2^x \hat{\tau}_x, \quad \Phi_0^x = \phi_0^x, \quad \begin{pmatrix} \Phi_1^x \\ \Phi_2^x \end{pmatrix} = \begin{bmatrix} \cos \theta_{\mathbf{k}} & -\sin \theta_{\mathbf{k}} \\ \sin \theta_{\mathbf{k}} & \cos \theta_{\mathbf{k}} \end{bmatrix} \begin{pmatrix} \phi_1^x \\ \phi_2^x \end{pmatrix} \quad (32)$$

Similarly, we find

$$\begin{aligned} \hat{U}_{\mathbf{k}}^{-1} (\hat{\phi}^y(\mathbf{k}) \otimes \hat{\sigma}_y) \hat{U}_{\mathbf{k}} &= \hat{\Phi}^y(\mathbf{k}) \otimes \hat{\sigma}_y, \quad \hat{U}_{\mathbf{k}}^{-1} (\hat{\phi}^z(\mathbf{k}) \otimes \hat{\sigma}_z) \hat{U}_{\mathbf{k}} = \hat{\Phi}^z(\mathbf{k}) \otimes \hat{\sigma}_z, \\ \hat{\Phi}^y &= \Phi_0^y \hat{\tau}_0 + \Phi_1^y \hat{\tau}_z + \Phi_2^y \hat{\tau}_x, \quad \Phi_0^y = \phi_0^y, \quad \begin{pmatrix} \Phi_1^y \\ \Phi_2^y \end{pmatrix} = \begin{bmatrix} \cos \theta_{\mathbf{k}} & \sin \theta_{\mathbf{k}} \\ -\sin \theta_{\mathbf{k}} & \cos \theta_{\mathbf{k}} \end{bmatrix} \begin{pmatrix} \phi_1^y \\ \phi_2^y \end{pmatrix}, \\ \hat{\Phi}^z &= \Phi_0^z \hat{\tau}_0 + \Phi_1^z \hat{\tau}_z + \Phi_2^z \hat{\tau}_x, \quad \Phi_0^z = \phi_0^z, \quad \begin{pmatrix} \Phi_1^z \\ \Phi_2^z \end{pmatrix} = \begin{bmatrix} \cos \theta_{\mathbf{k}} & -\sin \theta_{\mathbf{k}} \\ \sin \theta_{\mathbf{k}} & \cos \theta_{\mathbf{k}} \end{bmatrix} \begin{pmatrix} \phi_1^z \\ \phi_2^z \end{pmatrix}. \end{aligned} \quad (33)$$

Thus, we can re-write (25) as follows

$$\tilde{H}_V = iV_{df} \frac{b}{2} \sum_{\mathbf{k}} \hat{d}_{\mathbf{k}\alpha}^\dagger [\hat{\Phi}_{\mathbf{k}}]_{\alpha\beta} \tilde{f}_{\mathbf{k}\beta} + \text{h.c.}, \quad \hat{\Phi}_{\mathbf{k}} = \hat{\Phi}^x(\mathbf{k}) \otimes \hat{\sigma}_x + \hat{\Phi}^y(\mathbf{k}) \otimes \hat{\sigma}_y + \hat{\Phi}^z(\mathbf{k}) \otimes \hat{\sigma}_z \quad (34)$$

Next we derive the mean-field equations.

### Derivation of the mean-field equations

To derive the mean field equations we first integrate out  $d$ -electrons by making the following change of variables in the path integral:

$$\begin{aligned} \hat{d}_{\mathbf{k}}^\dagger &\rightarrow \hat{d}_{\mathbf{k}}^\dagger + \hat{f}_{\mathbf{k}}^\dagger \hat{\Phi}_{\mathbf{k}}^\dagger \hat{G}_d(i\omega, \mathbf{k}), \quad \hat{d}_{\mathbf{k}} \rightarrow \hat{d}_{\mathbf{k}} + \hat{G}_d(i\omega, \mathbf{k}) \hat{\Phi}_{\mathbf{k}} \hat{f}_{\mathbf{k}}, \\ \hat{G}_d^{-1}(i\omega, \mathbf{k}) &= \begin{pmatrix} i\omega - E_{1\mathbf{k}}^{(d)} & 0 & 0 & 0 \\ 0 & i\omega - E_{1\mathbf{k}}^{(d)} & 0 & 0 \\ 0 & 0 & i\omega - E_{2\mathbf{k}}^{(d)} & 0 \\ 0 & 0 & 0 & i\omega - E_{2\mathbf{k}}^{(d)} \end{pmatrix}. \end{aligned} \quad (35)$$

Then the resulting action is Gaussian and the  $f$ -electrons can be integrated out. This yields the effective action of the form

$$S_{eff} = (b^2 - 1)(E_f - \varepsilon_f) - T \sum_{i\omega} \sum_{\mathbf{k}} \log \det \left[ \hat{G}_{ff}^{-1}(i\omega, \mathbf{k}) \right], \quad \hat{G}_{ff}^{-1} = \hat{G}_f^{-1}(i\omega, \mathbf{k}) - (V_{df} \frac{b}{2})^2 \hat{\Phi}_{\mathbf{k}}^\dagger \hat{G}_d(i\omega, \mathbf{k}) \hat{\Phi}_{\mathbf{k}}. \quad (36)$$

The renormalized  $f$ -electron correlation function  $\hat{G}_{ff}^{-1}$  has a block diagonal form:

$$\hat{G}_{ff}^{-1} = \frac{(V_{df} b)^2}{4} \begin{pmatrix} \mathcal{G}_{1f}^{-1}(i\omega, \mathbf{k}) \frac{4}{(V_{df} b)^2} & 0 & -\frac{\Delta_{1\mathbf{k}}}{i\omega - E_{1\mathbf{k}}^{(d)}} - \frac{\Delta_{2\mathbf{k}}}{i\omega - E_{2\mathbf{k}}^{(d)}} & -\frac{\tilde{\Delta}_{1\mathbf{k}}}{i\omega - E_{1\mathbf{k}}^{(d)}} - \frac{\tilde{\Delta}_{2\mathbf{k}}}{i\omega - E_{2\mathbf{k}}^{(d)}} \\ 0 & \mathcal{G}_{1f}^{-1}(i\omega, \mathbf{k}) \frac{4}{(V_{df} b)^2} & \frac{\tilde{\Delta}_{1\mathbf{k}}}{i\omega - E_{1\mathbf{k}}^{(d)}} + \frac{\tilde{\Delta}_{2\mathbf{k}}}{i\omega - E_{2\mathbf{k}}^{(d)}} & -\frac{\Delta_{1\mathbf{k}}}{i\omega - E_{1\mathbf{k}}^{(d)}} - \frac{\Delta_{2\mathbf{k}}}{i\omega - E_{2\mathbf{k}}^{(d)}} \\ -\frac{\Delta_{1\mathbf{k}}}{i\omega - E_{1\mathbf{k}}^{(d)}} - \frac{\Delta_{2\mathbf{k}}}{i\omega - E_{2\mathbf{k}}^{(d)}} & \frac{\tilde{\Delta}_{1\mathbf{k}}}{i\omega - E_{1\mathbf{k}}^{(d)}} + \frac{\tilde{\Delta}_{2\mathbf{k}}}{i\omega - E_{2\mathbf{k}}^{(d)}} & \mathcal{G}_{2f}^{-1}(i\omega, \mathbf{k}) \frac{4}{(V_{df} b)^2} & 0 \\ -\frac{\tilde{\Delta}_{1\mathbf{k}}}{i\omega - E_{1\mathbf{k}}^{(d)}} - \frac{\tilde{\Delta}_{2\mathbf{k}}}{i\omega - E_{2\mathbf{k}}^{(d)}} & -\frac{\Delta_{1\mathbf{k}}}{i\omega - E_{1\mathbf{k}}^{(d)}} - \frac{\Delta_{2\mathbf{k}}}{i\omega - E_{2\mathbf{k}}^{(d)}} & 0 & \mathcal{G}_{2f}^{-1}(i\omega, \mathbf{k}) \frac{4}{(V_{df} b)^2} \end{pmatrix}, \quad (37)$$

where the diagonal elements are given by

$$\begin{aligned} \mathcal{G}_{1f}^{-1}(i\omega, \mathbf{k}) &= i\omega - E_{1\mathbf{k}}^{(f)} - (V_{df} \frac{b}{2})^2 \left[ \frac{\Phi_{1\mathbf{k}}^{(+)}}{i\omega - E_{1\mathbf{k}}^{(d)}} + \frac{\Phi_{2\mathbf{k}}}{i\omega - E_{2\mathbf{k}}^{(d)}} \right], \\ \mathcal{G}_{2f}^{-1}(i\omega, \mathbf{k}) &= i\omega - E_{2\mathbf{k}}^{(f)} - (V_{df} \frac{b}{2})^2 \left[ \frac{\Phi_{2\mathbf{k}}}{i\omega - E_{1\mathbf{k}}^{(d)}} + \frac{\Phi_{1\mathbf{k}}^{(-)}}{i\omega - E_{2\mathbf{k}}^{(d)}} \right], \end{aligned} \quad (38)$$

and we have introduced the following functions

$$\begin{aligned}
\Phi_{1\mathbf{k}}^{(\pm)} &= (\Phi_0^x \pm \Phi_1^x)^2 + (\Phi_0^y \pm \Phi_1^y)^2 + (\Phi_0^z \pm \Phi_1^z)^2, & \Phi_{2\mathbf{k}} &= (\Phi_2^x)^2 + (\Phi_2^y)^2 + (\Phi_2^z)^2, \\
\Delta_{1\mathbf{k}} &= \Phi_2^z(\Phi_0^z + \Phi_1^z) + (\Phi_2^x + i\Phi_2^y)[\Phi_0^x + \Phi_1^x - i(\Phi_0^y + \Phi_1^y)], \\
\Delta_{2\mathbf{k}} &= \Phi_2^z(\Phi_0^z - \Phi_1^z) + (\Phi_2^x - i\Phi_2^y)[\Phi_0^x - \Phi_1^x + i(\Phi_0^y - \Phi_1^y)], \\
\tilde{\Delta}_{1\mathbf{k}} &= (\Phi_2^x - i\Phi_2^y)(\Phi_0^z + \Phi_1^z) - \Phi_2^z[\Phi_0^x + \Phi_1^x - i(\Phi_0^y + \Phi_1^y)], \\
\tilde{\Delta}_{2\mathbf{k}} &= \Phi_2^z[\Phi_0^x - \Phi_1^x - i(\Phi_0^y - \Phi_1^y)] - (\Phi_2^x - i\Phi_2^y)(\Phi_0^z - \Phi_1^z).
\end{aligned} \tag{39}$$

Then the determinant of the matrix  $\hat{G}_{ff}$  is

$$\begin{aligned}
\det \left[ \hat{G}_{ff}^{-1}(i\omega, \mathbf{k}) \right] &= \left\{ \mathcal{G}_{1f}^{-1}(i\omega, \mathbf{k}) \mathcal{G}_{2f}^{-1}(i\omega, \mathbf{k}) - (V_{df} \frac{b}{2})^4 \left( \frac{\Delta_{1\mathbf{k}}}{i\omega - E_{1\mathbf{k}}^{(d)}} + \frac{\Delta_{2\mathbf{k}}}{i\omega - E_{2\mathbf{k}}^{(d)}} \right) \left( \frac{\Delta_{1\mathbf{k}}^*}{i\omega - E_{1\mathbf{k}}^{(d)}} + \frac{\Delta_{2\mathbf{k}}^*}{i\omega - E_{2\mathbf{k}}^{(d)}} \right) \right. \\
&\quad \left. - (V_{df} \frac{b}{2})^4 \left( \frac{\tilde{\Delta}_{1\mathbf{k}}}{i\omega - E_{1\mathbf{k}}^{(d)}} + \frac{\tilde{\Delta}_{2\mathbf{k}}}{i\omega - E_{2\mathbf{k}}^{(d)}} \right) \left( \frac{\tilde{\Delta}_{1\mathbf{k}}^*}{i\omega - E_{1\mathbf{k}}^{(d)}} + \frac{\tilde{\Delta}_{2\mathbf{k}}^*}{i\omega - E_{2\mathbf{k}}^{(d)}} \right) \right\}^2.
\end{aligned} \tag{40}$$

Furthermore, we find that

$$|\Delta_{1\mathbf{k}}|^2 + |\tilde{\Delta}_{1\mathbf{k}}|^2 = \Phi_{1\mathbf{k}}^{(+)} \Phi_{2\mathbf{k}}, \quad |\Delta_{2\mathbf{k}}|^2 + |\tilde{\Delta}_{2\mathbf{k}}|^2 = \Phi_{1\mathbf{k}}^{(-)} \Phi_{2\mathbf{k}} \tag{41}$$

so that certain terms in the expression (40) will cancel. Therefore, to derive the mean field equation we will need to find the saddle point of the following effective action:

$$S_{eff} = (b^2 - 1)(E_f - \varepsilon_f) - 2T \sum_{i\omega} \sum_{\mathbf{k}} \log[P_{4\mathbf{k}}(i\omega; E_f, b)], \quad P_{4\mathbf{k}}(i\omega) = \prod_{i=1}^4 (i\omega - \varepsilon_{i\mathbf{k}}). \tag{42}$$

where we have introduced the polynomial:

$$\begin{aligned}
P_{4\mathbf{k}}(i\omega) &= (i\omega - E_{1\mathbf{k}}^{(f)})(i\omega - E_{2\mathbf{k}}^{(f)})(i\omega - E_{1\mathbf{k}}^{(d)})(i\omega - E_{2\mathbf{k}}^{(d)}) + (V_{df} \frac{b}{2})^4 \gamma_{\mathbf{k}}^4 - \\
&\quad - (V_{df} \frac{b}{2})^2 \left\{ [\Phi_{2\mathbf{k}}(i\omega - E_{1\mathbf{k}}^{(f)}) + \Phi_{1\mathbf{k}}^+(i\omega - E_{2\mathbf{k}}^{(f)})](i\omega - E_{2\mathbf{k}}^{(d)}) + [\Phi_{2\mathbf{k}}(i\omega - E_{2\mathbf{k}}^{(f)}) + \Phi_{1\mathbf{k}}^-(i\omega - E_{1\mathbf{k}}^{(f)})](i\omega - E_{1\mathbf{k}}^{(d)}) \right\}, \\
\gamma_{\mathbf{k}}^4 &= \Phi_{1\mathbf{k}}^+ \Phi_{1\mathbf{k}}^- + \Phi_{2\mathbf{k}}^2 - \Delta_{1\mathbf{k}} \Delta_{2\mathbf{k}}^* - \Delta_{1\mathbf{k}}^* \Delta_{2\mathbf{k}} - \tilde{\Delta}_{1\mathbf{k}} \tilde{\Delta}_{2\mathbf{k}}^* - \tilde{\Delta}_{1\mathbf{k}}^* \tilde{\Delta}_{2\mathbf{k}}.
\end{aligned} \tag{43}$$

Thus, two of the three mean field equations are formally given by

$$\frac{\partial S_{eff}}{\partial E_f} = 0, \quad \frac{\partial S_{eff}}{\partial b} = 0. \tag{44}$$

We have

$$b^2 - 1 + 2 \sum_{i=1}^4 \sum_{\mathbf{k}} \frac{f(\varepsilon_{i\mathbf{k}}) n_F(\varepsilon_{i\mathbf{k}})}{\prod_{l \neq i} (\varepsilon_{i\mathbf{k}} - \varepsilon_{l\mathbf{k}})} = 0, \quad n_F(x) = \frac{1}{e^{\beta x} + 1}, \tag{45}$$

where the function  $f(\varepsilon)$  is:

$$\begin{aligned}
f(\lambda) &= 2\lambda^3 - \lambda^2 [2(E_{1\mathbf{k}}^{(d)} + E_{2\mathbf{k}}^{(d)}) + E_{1\mathbf{k}}^{(f)} + E_{2\mathbf{k}}^{(f)}] \\
&\quad + \lambda [2E_{1\mathbf{k}}^{(d)} E_{2\mathbf{k}}^{(d)} + (E_{1\mathbf{k}}^{(d)} + E_{2\mathbf{k}}^{(d)})(E_{1\mathbf{k}}^{(f)} + E_{2\mathbf{k}}^{(f)}) - (V_{df} \frac{b}{2})^2 (\Phi_{1\mathbf{k}}^+ + \Phi_{1\mathbf{k}}^- + 2\Phi_{2\mathbf{k}})] \\
&\quad + (V_{df} \frac{b}{2})^2 [(\Phi_{2\mathbf{k}} + \Phi_{1\mathbf{k}}^-) E_{1\mathbf{k}}^{(d)} + (\Phi_{2\mathbf{k}} + \Phi_{1\mathbf{k}}^+) E_{2\mathbf{k}}^{(d)}] - E_{1\mathbf{k}}^{(d)} E_{2\mathbf{k}}^{(d)} (E_{1\mathbf{k}}^{(f)} + E_{2\mathbf{k}}^{(f)})
\end{aligned} \tag{46}$$

The derivation of the last mean-field equation can be compactly written as follows:

$$8(E_f - \varepsilon_f) + 2 \sum_{i=1}^4 \sum_{\mathbf{k}} \frac{\partial \varepsilon_{i\mathbf{k}}}{\partial E_f} n_F(\varepsilon_{i\mathbf{k}}) = 0. \tag{47}$$